

## PHOTOCURRENT IN THE SUB BANDGAP REGION OF A-SI:H PHOTSENSITIVE DEVICES INDUCED BY AG NANOPARTICLES

F. Lükermann<sup>1</sup>, U. Heinzmann<sup>1</sup> and H. Stiebig<sup>1,2</sup>

<sup>1</sup>Molecular and Surface Physics, University of Bielefeld, Universitätsstr. 25, D-33615 Bielefeld, Germany,  
Phone: +49(521)106-5471, Fax: +49(521)106-6001, email: [florian.luekermann@physik.uni-bielefeld.de](mailto:florian.luekermann@physik.uni-bielefeld.de)

<sup>2</sup>Malibu GmbH & Co. KG, Böttcherstr. 7, D-33609 Bielefeld, Germany,  
Phone: +49(521)9892880, Fax: +49(521)98928813, email: [hstiebig@schueco.com](mailto:hstiebig@schueco.com)

**ABSTRACT:** In this contribution the absorption by defect states in hydrogenated amorphous silicon (a-Si:H) photosensitive devices in the environment of resonant absorbing silver nanoparticles (Ag NPs) is investigated. The location of defects in the strong electromagnetic fields accompanied by the localized surface plasmon (LSP) resonance of the Ag NPs enable high transition rates between the defect states and the conduction band. This results in a significant signal for near infrared (NIR) photon energies in external quantum efficiency (EQE) measurements. Dominant transitions take place for defect levels with an energetic distance from the conduction band, equal to the LSP resonance energy.

Introducing a boron doped layer in direct contact to the NPs leads to a decrease of the NIR EQE signal. This gives evidence for the existence of the NP induced defect states in the a-Si:H material. The p-type doping shifts the Fermi level towards or below the defect states resulting in their depletion. Therefore these states cannot contribute to sub bandgap photon absorption resulting in a decreased NIR EQE signal.

**Keywords:** localized surface plasmon resonance, silver nanoparticles, hydrogenated amorphous silicon, sub bandgap photocurrent, impurity photovoltaic effect, resonant defect absorption

### 1 INTRODUCTION

Efficient thin film silicon solar cell devices rely on the utilization of a broad portion of the solar spectral radiation. Especially wasting of sub bandgap photons is a major loss mechanism for solar cells. The quasi direct bandgap of hydrogenated amorphous silicon (a-Si:H) at 1.7 eV enables strong absorption for the visible spectral region. While red and near infrared (NIR) light is not absorbed efficiently.

To take advantage of a broader spectral range different approaches are made. Tandem or multi-junction solar cells composed of a-Si:H, amorphous silicon germanium (a-SiGe:H) based alloys, micro-crystalline silicon ( $\mu$ c-Si:H) and combinations thereof are investigated [1,2]. These materials in conjunction cover a broader range of the solar spectrum due to their different bandgaps. A different approach is the use of sub bandgap light by photon up-conversion [3] where low energy photons are transformed to high energy photons that can excite electronic transitions between the band edges of the absorber. Here the up converter is electrically isolated from the absorber layer. Similar to this approach is the impurity photovoltaic effect (IPV). This effect enables the excitation from the valence to the conduction band by a two step excitation via a defect state in the bandgap of the absorber. Theoretical studies predict a benefit for the performance of solar cells by making use of the IPV effect [4], also in amorphous silicon solar cells [5]. However, the benefit of this effect is discussed controversially by others [6], mainly due to increased recombination via the defect levels.

Beside this, the application of metal nanostructures to solar cell devices has found increasing interest for enhancing the photon absorption. Here localized surface plasmon (LSP) resonances that are excited upon interaction between electromagnetic radiation with the

metal nanostructures are investigated. Mostly the ability of large metal nanostructures (in the range of hundreds of nanometers) to scatter light is used in order to enhance the optical thickness of solar absorber layers [7,8]. Apart from this light trapping approach dominated by scattering, the use of small silver nanoparticles (Ag NPs) is investigated. It has been demonstrated in previous contributions that the application of approximately 20 nm Ag NPs to the interface of Schottky structures composed of a-Si:H and transparent conductive oxide (TCO) layers [9,10] or inside the intrinsic layer of a-Si:H n-i-p structures [10] yields a photocurrent for photon energies below the bandgap of the a-Si:H absorber. This is assigned to the creation of defect states in the a-Si:H material due to the presence of the silver nanoparticles in the a-Si:H network, implicitly interface defects or impurities caused by silver atoms. These states lie within the a-Si:H bandgap. Because the defects are created in direct vicinity of the strongly resonant absorbing Ag NPs, they are exposed to the strong electromagnetic fields in their environment going along with the LSP resonances. These strong fields promote resonant defect absorption with high transition rates between the created defect states and the band edges. Therefore this finding is a demonstration for the use of the IPV effect in a-Si:H devices [10].

By using different particle size distributions a shift of the dominant EQE response in the NIR regime is observed [11]. This is correlated to the shift of the LSP resonance energy that addresses different defect levels for the resonant transitions to the band edges.

In this contribution the influence of Ag NP environment on the generated photocurrent for photon energies in the NIR is investigated, especially with respect to doping of a-Si:H in the NP environment. A varying boron doping concentration is expected to shift the Fermi level towards the valence band and should

probe the energetic position as well as the nature of the IPV introduced defect states.

## 2 EXPERIMENTAL

Ag NPs are incorporated in a-Si:H photosensitive devices (see Figure 1 (a)). Thin film deposition is mainly carried out in industry sized deposition facilities on glass substrates with a dimension of 1.4 m<sup>2</sup>. Fabricated devices are composed of a glass substrate with a front TCO, either a 1 μm thick sputter deposited Al:ZnO (AZO) or a standard Asahi SnO<sub>2</sub>. The a-Si:H layers are deposited by plasma enhanced chemical vapor deposition (PECVD). Very thin intrinsic absorber layers (30 nm) are used to enable a strong build in electrostatic field for efficient charge carrier extraction. The Ag NPs are prepared by sputtering of silver films with a few nanometers thickness. Afterwards the silver films are annealed in vacuum at temperatures between 150 °C and 200 °C for 30 min, resulting in the agglomeration of Ag NPs caused by surface tension. The silver films itself are deposited by DC magnetron sputtering on the large 1.4 m<sup>2</sup> substrate at room temperature and a pressure of 10<sup>-3</sup> mbar, or by dividing the substrate in 5x5 cm<sup>2</sup> samples prior to deposition and afterwards sputtering the silver films in an ultra high vacuum chamber at similar deposition conditions. In all cases, the NP size distribution can be altered by varying the silver film thickness.

The back contact applied in all devices is a combination of sputter deposited AZO and silver reflector layers with thicknesses of 80 nm and 100 nm, respectively. Devices with an active cell area of 1 cm<sup>2</sup> are defined by laser scribing.

The Fermi level  $E_F$  position with respect to the different p-doping concentrations is determined by measuring the dark conductivity of single layers. For this purpose a-Si:H layers with the same doping gas fluxes used for the cell experiments are deposited on quartz glass substrates with a layer thickness of approximately 250 nm (Figure 2 (a)). Afterwards coplanar metal electrodes are deposited on top of these layers by thermal evaporation. The samples are then placed in a high vacuum cryostat and heated up to 150 °C prior to conductivity measurements for at least one hour in order to remove surface adsorbates and the influence of the Staebler-Wronski effect. The dark conductivity  $\sigma_d$  is measured in the coplanar contact configuration at several temperatures from 150 °C downwards. For intrinsic or n-type a-Si:H the logarithm of  $\sigma_d$  can be expressed in the form:

$$k \cdot \ln(\sigma_d(T)) = k \cdot \ln(\sigma_0(T)) - \frac{E_C - E_F}{T}.$$

Here  $E_C$  is the conduction band energy,  $k$  is the Boltzmann constant,  $T$  is the temperature in Kelvin and  $\sigma_0$  is a conductivity prefactor. By plotting  $k \ln(\sigma_d)$  versus  $1/T$  and fitting the data by a straight line, one obtains the difference between conduction band and Fermi level ( $E_C - E_F$ ) as negative slope of the fit. For p-doped samples this procedure results in the distance of  $E_F$  to the valence band ( $E_F - E_V$ ). To calculate in each case the opposite value, i.e. ( $E_F - E_V$ ) for intrinsic or ( $E_C - E_F$ ) for p-doped samples one has to subtract the obtained value from the bandgap energy. The optical bandgap is calculated from UV-Vis measurements via Tauc's method by plotting

$(\alpha h\nu)^{1/2}$  versus the photon energy  $h\nu$  and extrapolating the linear part towards the abscissa.

## 3 RESULTS AND DISCUSSION

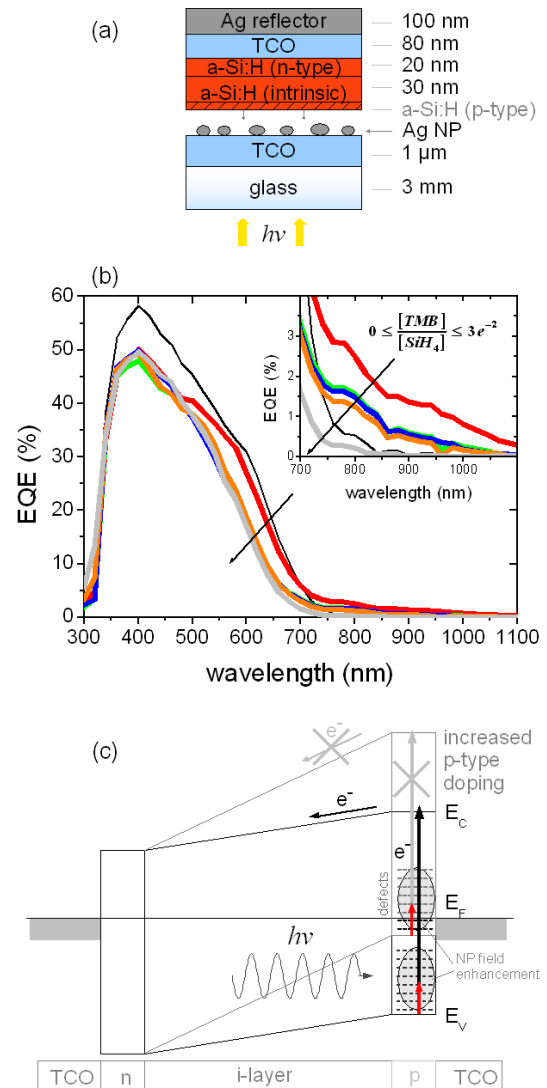


**Figure 1:** (a) Design of TCO/Ag NP/a-Si:H p-i-n/TCO Schottky structures with a varying doping concentration from intrinsic to highly p-doped at the front TCO/a-Si:H interface. Asahi SnO<sub>2</sub> is used as front TCO. (b) Measured influence of an increased p-type doping in the Ag NP environment on the EQE. The inset illustrates the characteristics in the NIR range with an enlarged ordinate scale. The tendency of an increased doping concentration in the gas mixture varying between  $[TMB]/[SiH_4]=0$  (i-n device) to  $[TMB]/[SiH_4] = 3 \cdot 10^{-2}$  (highly doped p-i-n device) is indicated by the arrows. (c) Possible explanation for decreasing EQE in the NIR range with increasing p-doping concentration. The increased p-type doping shifts  $E_V$  towards  $E_F$ , leading to a shift of defect levels above  $E_F$ . Consequently the levels are depleted and no charge carriers are available for resonant absorption processes.

The approach for the sub bandgap excitation by resonant defect absorption from the vicinity of the Ag NPs relies, for the case of an a-Si:H i-n structure, on the fact that the created defect states are occupied by electrons. The LSP resonance of Ag NPs provides strong fields in their environment at the defect locations leading to high transition rates from the defect levels. Charge compensation is carried out by thermal contact of the valence band to the defect states.

To investigate the nature of the defect states inside the a-Si:H bandgap and to test the proposed model, a p-doped layer is introduced in direct neighborhood to the NPs. By varying the doping concentration of this adjacent layer, the influence of the Fermi level shift on the defect absorption is investigated. A TCO/AgNP/a-Si:H p-i-n/TCO structure is build (Figure 1 (a)). The p-doping concentration is varied for different samples by changing the gas flow of Trimethylborane  $B(CH_3)_3$  (TMB) during the p-layer deposition. The ratio of TMB to Silane ( $SiH_4$ ) denoted as  $[TMB]/[SiH_4]$  is varied from 0 (undoped) for the reference sample to  $3 \cdot 10^{-2}$  (highly doped). The intrinsic layer thickness of the device without p-doped layer was about 30 nm. The introduced p-doped layer in all cases has a thickness of around 5 nm while the i-layer thickness is reduced to 25 nm. For all a-Si:H based devices, the total absorber layer thickness was kept constant. The front TCO in these devices is an Asahi  $SnO_2$ . For the experiments Ag NP dispersions of  $(23 \pm 9)$  nm (see Figure 3) are used.

EQE measurements of the devices are shown in Figure 1 (b). Due to the small absorber layer thickness, a maximum EQE signal of 55 to 60 % is measured for the i-n reference device (thin black line) without Ag NPs and without a p-doped layer. For NIR photons above 750 nm no photocurrent response is measured. By incorporating Ag NPs (thick red curve) to the i-n device a decreased signal is observed in the visible range. This is related to damping losses at the metal nanoparticles, leading to a lower amount of transmitted energy to the a-Si:H absorber.

For photon energies in the NIR (inset in Figure 1 (b)) two main findings can be made. First, the incorporation of Ag NPs leads to a significant EQE signal. A dominant shoulder at around 800 nm is observed that decreases towards the low energy part of the spectrum. The second finding is a decreasing EQE signal with increasing p-layer doping in the NP environment. The trend of EQE with an increasing doping concentration for samples with Ag NPs (thick curves) is indicated by the black arrows. The sample with highly doped p-layer shows a lower signal than the i-n reference device without Ag NPs. This trend is also evident for visible wavelengths above 500 nm where a decreased EQE signal is observed for the p-doped samples with respect to the undoped i-n device. The decreasing EQE signal with increasing p-type doping in the NP environment could be related to a shift of the Fermi level below the bandgap states. Therefore the Fermi level position in p-doped a-Si:H layers with the used doping gas ratios is measured as described above. Figure 2 (b) shows the distance of the valence and conduction band with respect to the Fermi level, which is set to zero in this diagram. The Tauc bandgap as the difference between  $E_C$  and  $E_V$  has a value of 1.75 eV for the intrinsic sample. For the lowest p-doping concentration the largest bandgap of around 2.1 eV is

measured. It decreases with increasing doping concentration to 1.9 eV mainly due to the role of  $H_2$  incorporation.

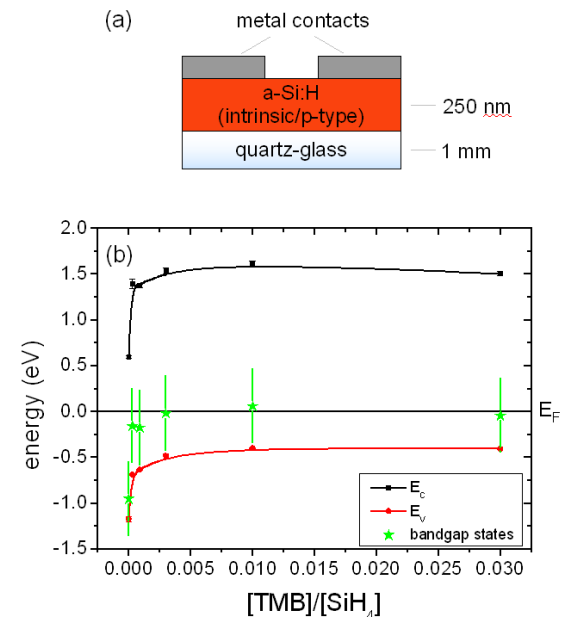


**Figure 2:** (a) Sample configuration for measurement of the dark conductivity for single a-Si:H layers with varying p-doping concentration. (b) Position of valence band (red dots) and conduction band (black squares) with respect to the Fermi Level (set to  $E_F=0$ ). The energetic positions and distances are derived from the optical Tauc bandgap and the distance of  $E_F$  to the band edges derived from the measured dark conductivity (see text). The measurements are carried out for single layer samples according to the doping concentration of the p-doped layers shown in Figure 1 (b).

The position of accessible bandgap states (green stars) is also shown. Their energetic position is deduced from the main contribution observed in the EQE measurement for the case of the i-n device with incorporated Ag NPs at roughly 800 nm (1.55 eV). It is plotted at each doping concentration relative to the conduction band. The error-bars indicate the width of the observable NIR EQE signal of around 0.4 eV especially towards the low energy region (up to 1100 nm (1.1 eV)). With an increased doping concentration a shift of the Fermi level towards the valence band and the defect states is observed. For medium and high doping concentrations the low energy part of the gap states is already shifted above  $E_F$  leading to a depletion of these states. This agrees with the observation of a decreasing EQE signal in the NIR, but cannot explain the complete disappearance of the NIR signal for the highest doping concentration of  $[TMB]/[SiH_4] = 3 \cdot 10^{-2}$ . This would require the Fermi level to shift completely below the accessible states. The measured Fermi level position for high doping concentrations might have to be reduced due to the statistical shift by roughly 200 meV [12]. The Fermi level would accordingly shift below the bandgap states leading to their depletion and consequently to a lack of an observable EQE signal for photons with sub bandgap energy. In any case the observed EQE NIR signal is sensitive to a shift of the Fermi level towards the

bandgap states. This is in agreement with the proposed defect states in the a-Si:H network due to the presence of the Ag NPs. When these states are depleted NIR photons cannot elevate electrons to the conduction band as illustrated in Figure 1 (c).

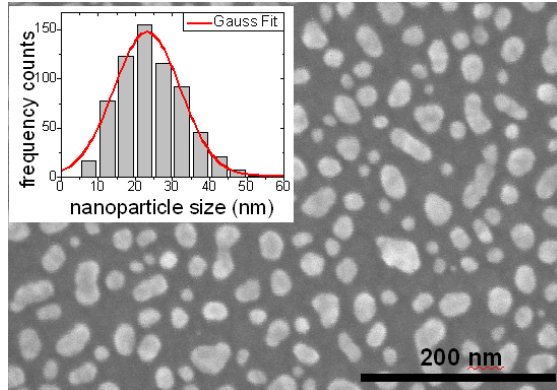


**Figure 3:** SEM image of the Ag NP size distribution with a mean particle diameter of 23 nm, used for all experiments within this contribution.

In addition other reasons could be of importance. The introduced doping increases the defect density by orders of magnitude and leads to increased recombination of charge carriers. Especially for those generated inside the p-layer, i.e. for electrons originating from the sub bandgap transitions near the NPs. Furthermore the NPs are outside the build in electrostatic field of the p-i-n diode. With an increased doping concentration the electrons generated in direct vicinity of the Ag NPs can be transported less efficient towards the n-layer.

#### 4 CONCLUSION

The effect of resonant defect absorption in a-Si:H photosensitive devices in the presence of Ag NPs is investigated. In particular the influence of the NP environment with respect to doping is investigated.

Introducing a p-type doping in direct environment of the Ag NPs leads to a decrease of the NIR EQE signal. One explanation for this observation could be the following. The introduced p-doping leads to a Fermi level shift towards the valence band resulting in a depletion of available defect states. Accordingly transitions from these states are not possible. This finding is an indication for the consistence of the proposed model of the resonant absorption from defect states close to the NPs.

The use of the sub bandgap defect absorption for solar cell applications seems to be limited in terms of the overall losses in the visible spectral region that are not overcompensated by the photocurrent for NIR photon energies. However the strong difference of the signal in the NIR between devices with and without Ag NPs in combination with the possibility to control the strength and spectral position by changing the NP size might be of interest for example in NIR detector applications. Additionally the freedom to take advantage of this effect in Schottky type devices or alternatively in p-i-n diodes [10] where the particles are embedded inside the intrinsic layer could be of interest in this context.

#### 5 REFERENCES

- [1] X. Deng, X. Liao, S. Han, H. Povolny, P. Agarwal, Amorphous silicon and silicon germanium materials for high-efficiency triple-junction solar cells, *Solar Energy Materials and Solar Cells* 62 (2000) 89 – 95.
- [2] H. Keppner, J. Meier, P. Torres, D. Fischer, A. Shah, Microcrystalline silicon and micromorph tandem solar cells, *Applied Physics A: Materials Science & Processing* 69 (1999) 169–177, 10.1007/s003390050987.
- [3] T. Trupke, M. A. Green, P. Würfel, Improving solar cell efficiencies by up-conversion of sub-band-gap light, *J. Appl. Phys.* 92 (7) (2002) 4117–4122.
- [4] M. Keevers, M. Green, Efficiency improvements of silicon solar cells by the impurity photovoltaic effect, *J. Appl. Phys.* 75 (8) (1994) 4022–4031.
- [5] H. Matsumura, H. Kasai, Theoretical study for drastic improvement of solar cell efficiency, *Japanese Journal of Applied Physics* 34 (Part 1, No. 5A) (1995) 2252–2259.
- [6] W. Shockley, H. J. Queisser, Detailed balance limit of efficiency of p-n junction solar cells, *J. Appl. Phys.* 32 (3) (1961) 510–519.
- [7] V. E. Ferry, M. A. Verschuuren, H. B. T. Li, E. Verhagen, R. J. Walters, R. E. I. Schropp, H. A. Atwater, A. Polman, Light trapping in ultrathin plasmonic solar cells, *Opt. Express* 18 (102) (2010) A237–A245.
- [8] S. Pillai, K. R. Catchpole, T. Trupke, M. A. Green, Surface plasmon enhanced silicon solar cells, *J. Appl. Phys.* 101 (2007) 093105.
- [9] E. Moulin, P. Q. Luo, B. Pieters, J. Sukmanowski, J. Kirchoff, W. Reetz, T. Müller, R. Carius, F. X. Royer, H. Stiebig, Photoresponse enhancement in the near infrared wavelength range of ultrathin amorphous silicon photosensitive devices by integration of silver nanoparticles, *Appl. Phys. Lett.* 95 (2009) 033505.
- [10] F. Lükermann, U. Heinzmann, H. Stiebig, Plasmon enhanced resonant defect absorption in thin a-Si:H n-i-p devices, *Appl. Phys. Lett.* 100 (25) (2012) 253907.
- [11] F. Lükermann, U. Heinzmann, H. Stiebig, Plasmon induced NIR response of thin-film a-Si:H solar cells, in: *Proceedings of SPIE*, Vol. 8471, 2012.
- [12] A. Shah, C. Droz, *Thin-film Silicon: Photovoltaics and Large-area Electronics*, EFPL Press, 2009.